Universität Rostock Traditio et Innovatio

Application of 2D Finite Integration Maxwell Solvers on Time Dependent and Eigenmode Problems

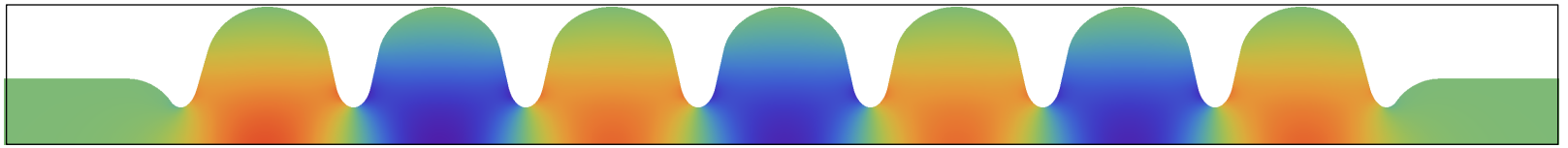

Mirjana Holst
12.12.2011, Rostock

- Introduction
- Finite Integration Technique (FIT) and preliminary considerations on FIT
- Eigenmode computation
- Time domain solver
- Comparison Mathematica code - MAFIA
- Cornell cavity
- Summary

Aim of the work:

- Creation of an algorithm which applies the Finite Integration Technique (FIT) on lossless 2D rotational symmetric structures
- Implementation of the FIT code in the scientific computing environment Mathematica
- Consistency and validation check of the performance of the new implementation
- Full and well elabourated documentation of the FIT code and the used internal procedures

General assumptions:

- Cylindrical coordinate system used (r,φ,z)
- TM_0 mode
- Equidistant grid, with the extension to non-equidistant grid
- Lossless system
- Electric boundary conditions

9-cell Tesla cavity

www.helmholtz-berlin.de/.../ hobicat/teslacav.jpg

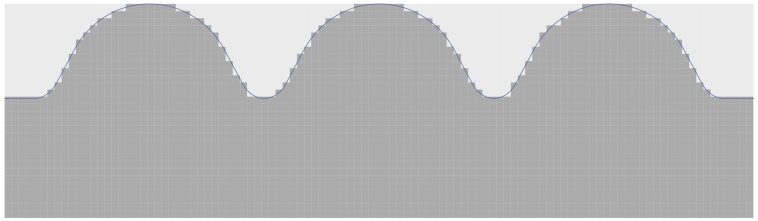

2D symmetric representation of 3-cells

Finite Integration Technique

FIT - discrete analogue of the Maxwell‘s equations

integral form

$$\oiint_{\partial V} \mathbf{D} \cdot \mathbf{dA} = \iiint_{V} \rho \cdot \mathbf{dV}$$ Gauss ‘ Law for electric fields

$$\oiint_{\partial V} \mathbf{B} \cdot \mathbf{dA} = 0$$ Gauss ‘ Law for magnetic fields

$$\oint_{\partial A} \mathbf{E} \cdot \mathbf{dl} = -\frac{\partial}{\partial t} \iint_{A} \mathbf{B} \cdot \mathbf{dA}$$ Faraday ‘s Law of Magnetic Induction

$$\oint_{\partial A} \mathbf{H} \cdot \mathbf{dl} = \iint_{A} \left(\frac{\partial}{\partial t} \mathbf{D} + \mathbf{J} \right) \cdot \mathbf{dA}$$ Ampère ‘s Law

T. Weiland: A Discretization Method for the Solution of Maxwell’s Equations for Six-Component Fields, Electronics and Communications AEÜ, vol. 31, no. 3, pp. 116–120, 1977.

Finite Integration Technique

FIT - discrete analogue of the Maxwell‘s equations

integral form

$$\oint_{\partial V} \mathbf{D} \cdot \mathbf{dA} = \iiint_{V} \rho \cdot \mathbf{dV}$$ Gauss ‘ Law for electric fields

$$\oint_{\partial V} \mathbf{B} \cdot \mathbf{dA} = 0$$ Gauss ‘ Law for magnetic fields

$$\oint_{\partial A} \mathbf{E} \cdot \mathbf{dl} = -\frac{\partial}{\partial t} \iint_{A} \mathbf{B} \cdot \mathbf{dA}$$ Faraday ‘s Law of Magnetic Induction

$$\oint_{\partial A} \mathbf{H} \cdot \mathbf{dl} = \iint_{A} \frac{\partial}{\partial t} \mathbf{D} \cdot \mathbf{dA}$$ Ampère ‘s Law

T. Weiland: A Discretization Method for the Solution of Maxwell’s Equations for Six-Component Fields, Electronics and Communications AEÜ, vol. 31, no. 3, pp. 116–120, 1977.

Finite Integration Technique

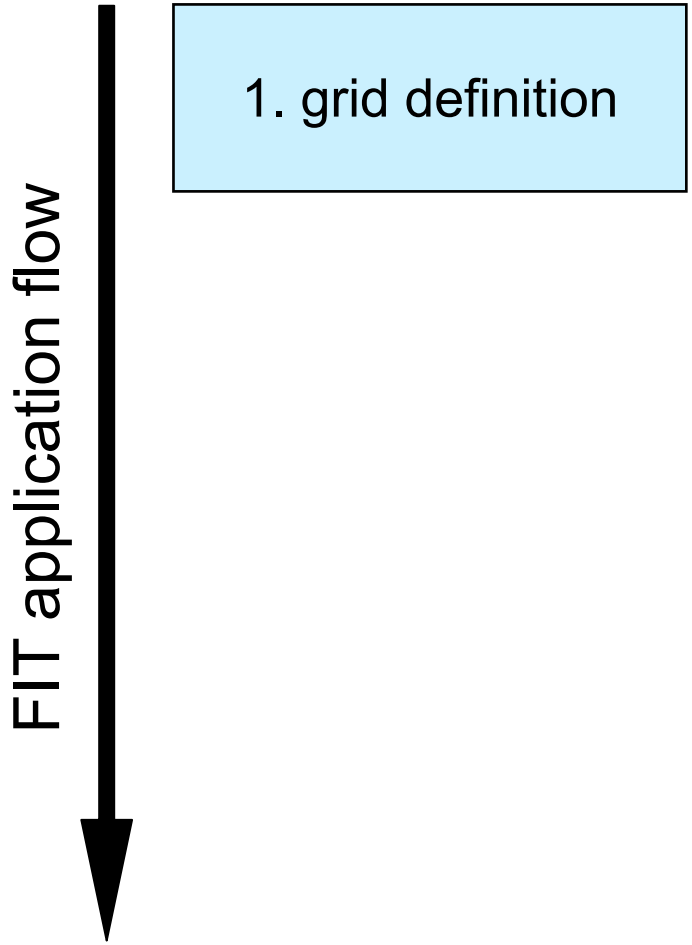

Finite Integration Technique

FIT application flow

1. grid definition

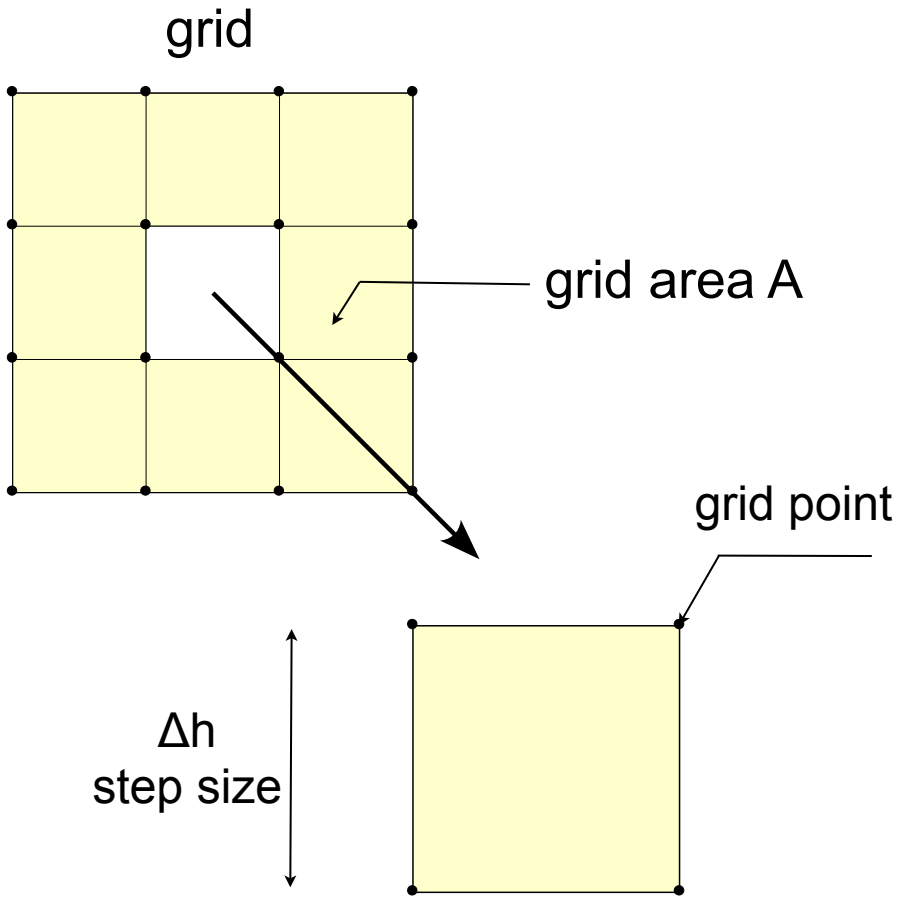

Finite Integration Technique

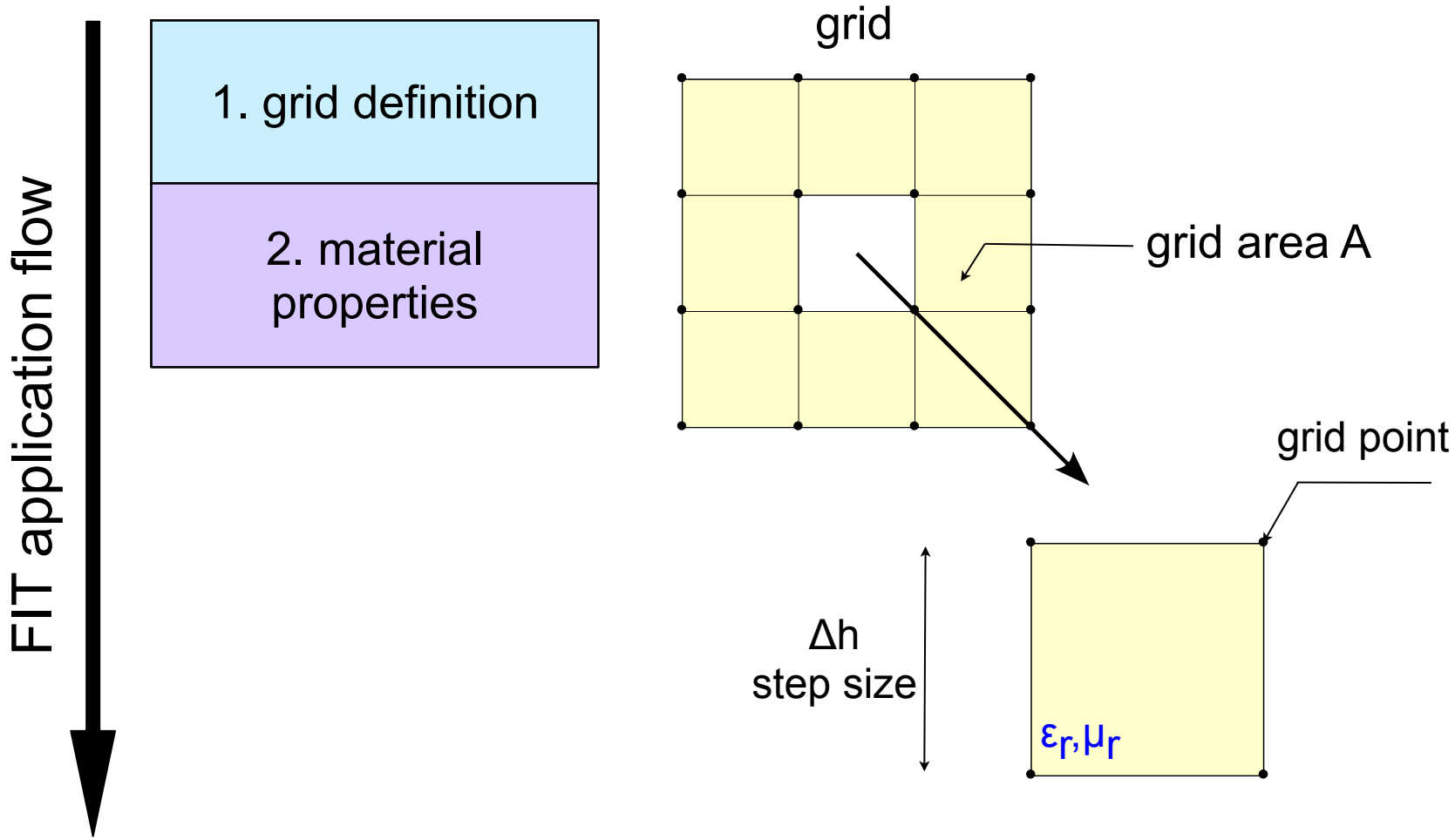

Finite Integration Technique

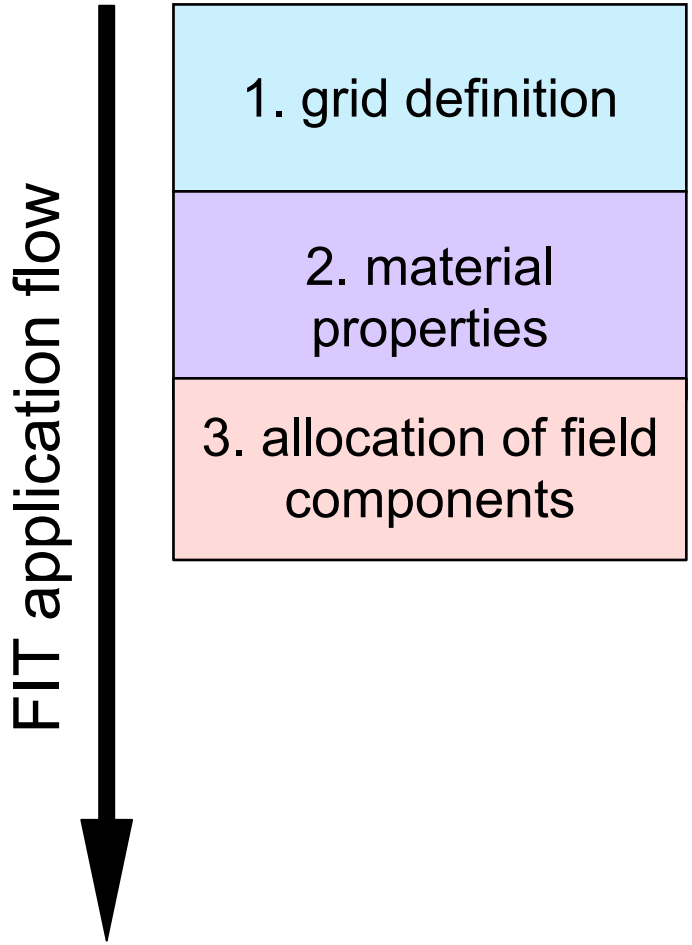

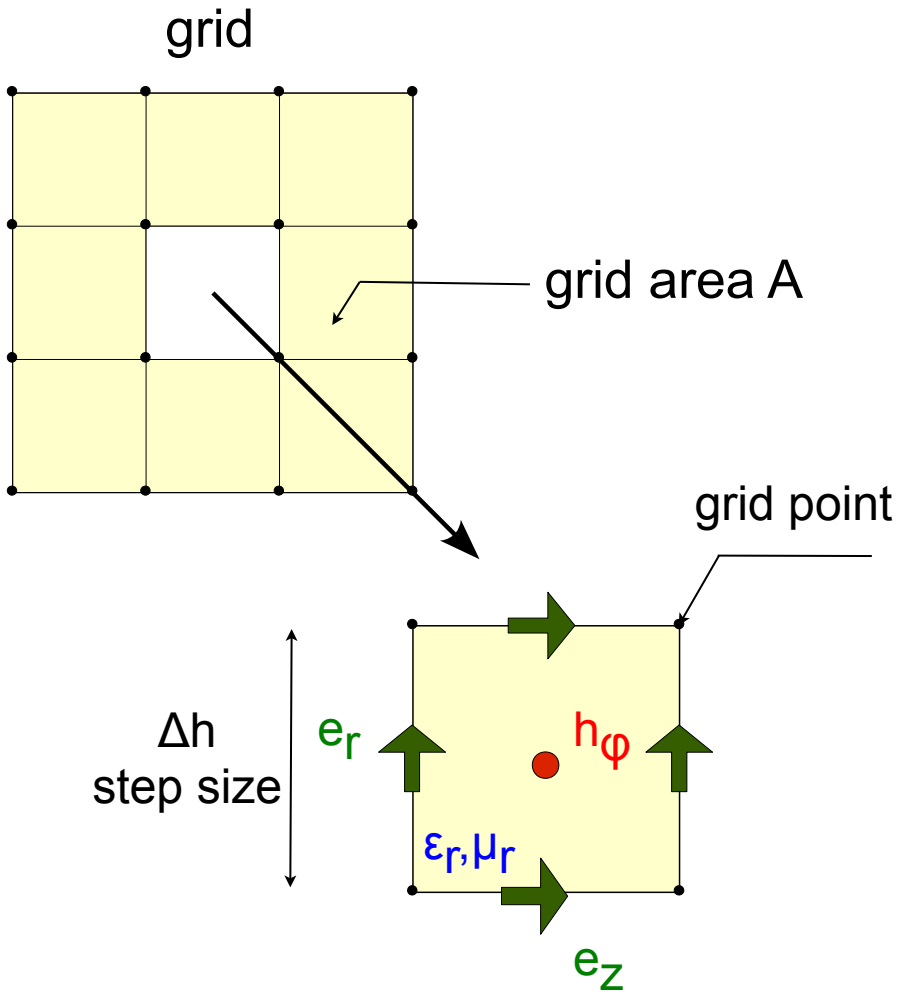

Finite Integration Technique

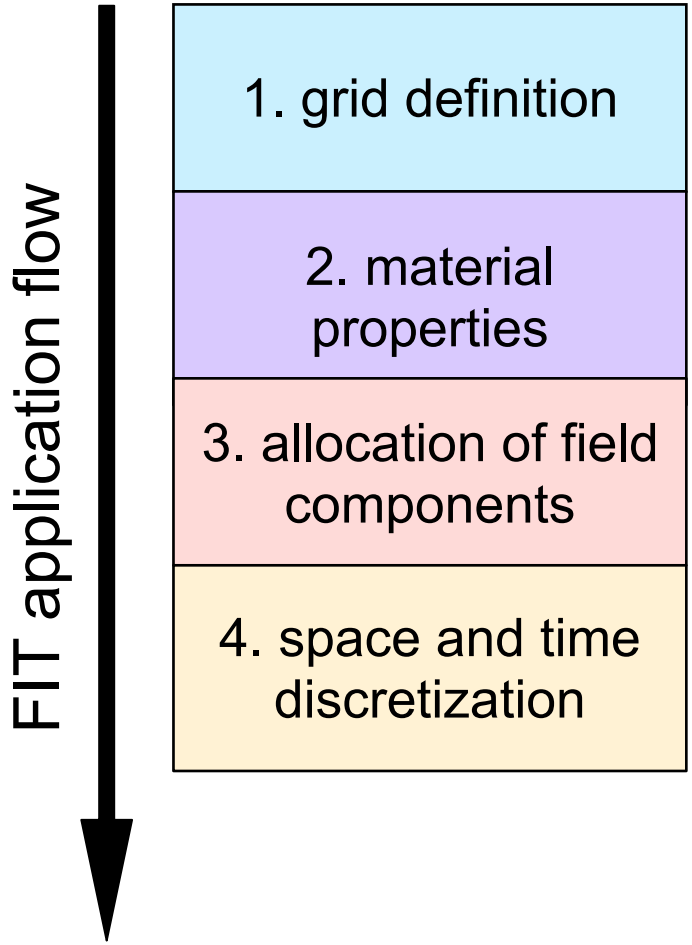

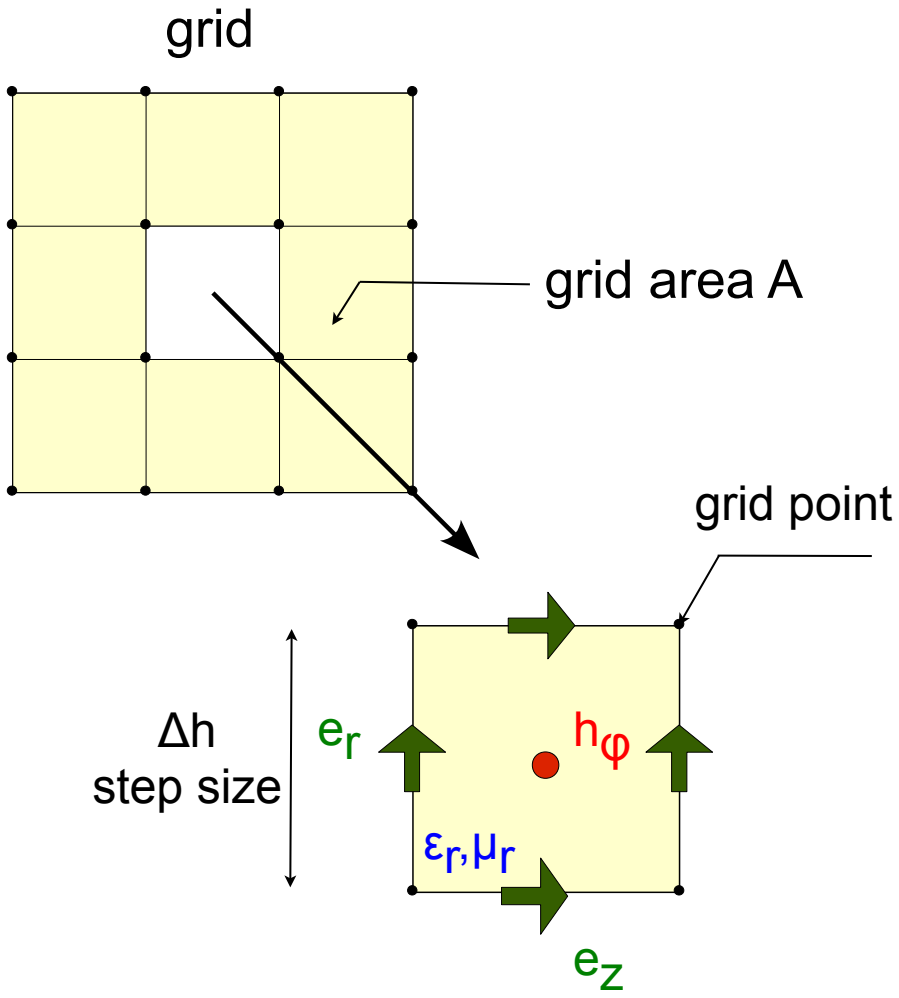

FIT: Space discretization of the Induction Law

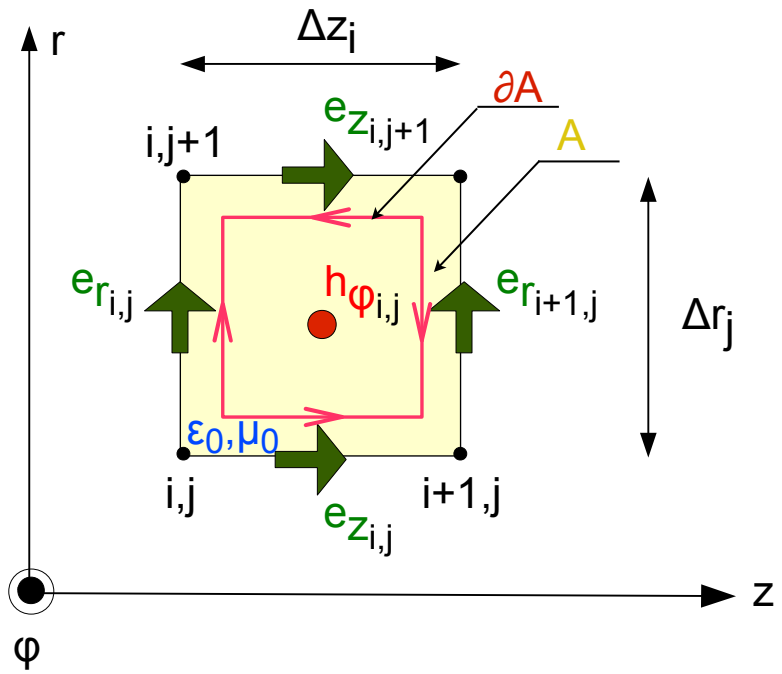

integral form

$$\oint_{\partial A} \mathbf{E}\cdot\mathbf{dl} = -\frac{\partial}{\partial t}\iint_{A} \mathbf{B}\cdot\mathbf{dA}$$

discrete form

$$\frac{\partial}{\partial t} h_{\varphi ij} = -\frac{1}{\mu_0}\left(\frac{e_{z ij}}{\Delta r_j} + \frac{e_{r i+1 j}}{\Delta z_i} - \frac{e_{z ij+1}}{\Delta r_j} - \frac{e_{r ij}}{\Delta z_i}\right)$$

Time discretization of Maxwell‘s equations

Replacement of the time derivatives by a central difference

$$\frac{\partial}{\partial t} e^{(n)} \approx \frac{e^{(n+1/2)} - e^{(n-1/2)}}{\Delta t}$$

$$\frac{\partial}{\partial t} h^{(n+1/2)} \approx \frac{h^{(n+1)} - h^{(n)}}{\Delta t}$$

Time step according to the ‘Courant-Friedrichs-Lewy (CFL) Condition

$$\Delta t \leq \min \left\{ \frac{\sqrt{\varepsilon_0 \mu_0}}{\sqrt{\frac{1}{\Delta z_i^2} + \frac{1}{\Delta r_j^2}}} \right\}$$

Δz - step width in z - direction
Δr - step width in r - direction

„Leap-frog“ scheme as time integration scheme

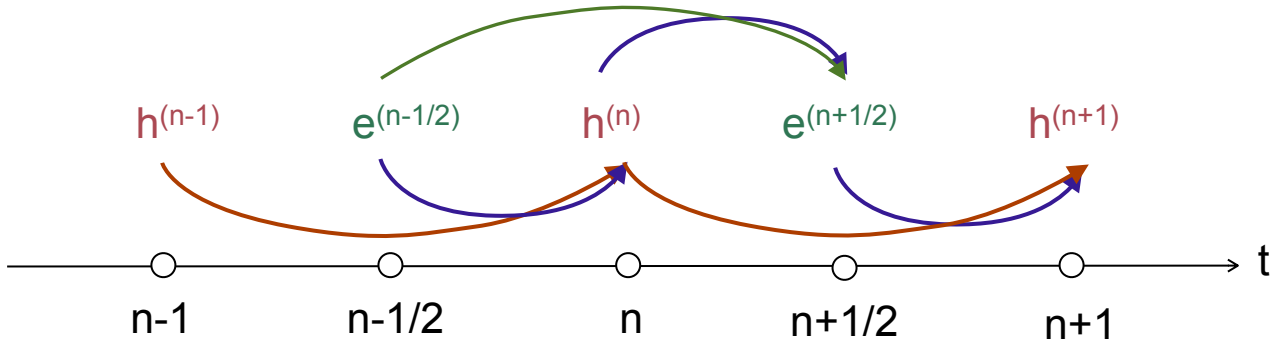

$$h_{\varphi_{ij}}^{(n+1)} = h_{\varphi_{ij}}^{(n)} - \frac{1}{\mu_0}\left(\frac{e_{z_{ij}}^{(n+1/2)}}{\Delta r_j} + \frac{e_{r_{i+1j}}^{(n+1/2)}}{\Delta z_i} - \frac{e_{z_{ij+1}}^{(n+1/2)}}{\Delta r_j} - \frac{e_{r_{ij}}^{(n+1/2)}}{\Delta z_i}\right)$$

$$e_{r_{ij}}^{(n+1/2)} = e_{r_{i+1j}}^{(n-1/2)} - \frac{1}{\varepsilon_0} \cdot \frac{2}{\Delta z_i + \Delta z_{i+1}} \left(h_{\varphi_{ij}}^{(n)} - h_{\varphi_{i+1j}}^{(n)}\right)$$

$$e_{z_{ij}}^{(n+1/2)} = e_{z_{ij}}^{(n-1/2)} - \frac{1}{\varepsilon_0} \cdot \frac{4}{\Delta r_j} h_{\varphi_{ij}}^{(n)}$$

Space and time discretized Maxwell's equations

$$h_\varphi^{(n+1)} = \begin{pmatrix} \mathbf{T_{11}} & \mathbf{T_{12}} & \mathbf{T_{13}} \end{pmatrix} \cdot \begin{pmatrix} h_\varphi^{(n)} \\ e_r^{(n+1/2)} \\ e_z^{(n+1/2)} \end{pmatrix}$$

$$\begin{pmatrix} e_r^{(n+1/2)} \\ e_z^{(n+1/2)} \end{pmatrix} = \begin{pmatrix} \mathbf{T_{21}} & \mathbf{T_{22}} & \mathbf{0} \\ \mathbf{T_{31}} & \mathbf{0} & \mathbf{T_{33}} \end{pmatrix} \cdot \begin{pmatrix} h_\varphi^{(n)} \\ e_r^{(n-1/2)} \\ e_z^{(n-1/2)} \end{pmatrix}$$

$$\begin{pmatrix} h_\varphi^{(n+1)} \\ e_r^{(n+1/2)} \\ e_z^{(n+1/2)} \end{pmatrix} = \underbrace{\begin{pmatrix} \mathbf{I}+\mathbf{T_{12}}\mathbf{T_{21}}+\mathbf{T_{13}}\mathbf{T_{31}} & \mathbf{T_{12}} & \mathbf{T_{13}} \\ \mathbf{T_{21}} & \mathbf{I} & \mathbf{0} \\ \mathbf{T_{31}} & \mathbf{0} & \mathbf{I} \end{pmatrix}}_{\text{System matrix}} \cdot \begin{pmatrix} h_\varphi^{(n)} \\ e_r^{(n-1/2)} \\ e_z^{(n-1/2)} \end{pmatrix}$$

T_{11}, T_{22}, T_{33} unit matrix (I)

Transformation from time to frequency domain

Using the Separation of variables for the solution of the Helmholtz‘ equation leads to:

$$\mathbf{F}(\mathbf{r},t) = \mathrm{Re}\left\{\mathbf{F}\left(\mathbf{r}\right)\cdot e^{j\omega t}\right\}$$

Differentiating and cancelling the exponential term on both sides of Maxwell‘s equations leads to

$$\frac{\partial}{\partial t} \rightarrow j\omega$$

i.e from the differential Maxwell grid equations in time domain, complex algebraic equations for the frequency domain can be derived

Eigenmode solver

An eigenmode solver computes resonant frequencies as well as their electromagnetic fields.

The equation to be solved is an eigenvalue problem and its eigenvalues correspond to the related eigenvectors (eigenmodes).

$$-\omega^2 \cdot h_\varphi = \mathbf{A} \cdot h_\varphi$$

Only few steps away from getting a consistent eigenmode solution

$\omega^2 + \lambda = 0 \quad \Rightarrow \quad \boxed{\omega^2 = -\lambda}$ the eigenvalues of the frequency matrix are negative and real

$\omega = 2\pi f \quad \Rightarrow \quad \boxed{f = (\sqrt{-\lambda}) / 2\pi}$ eigenfrequency calculation

Consistency check

- cylindrical cavity

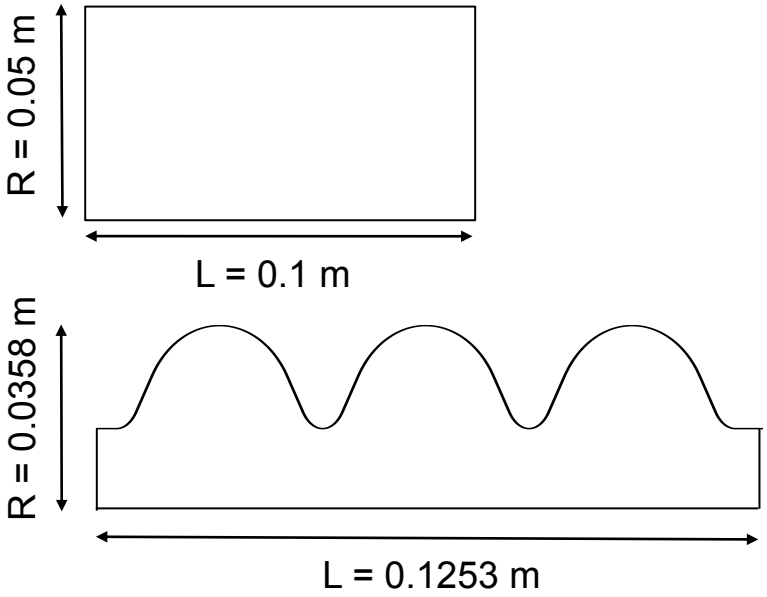

- cylindrical cavity with a pipe

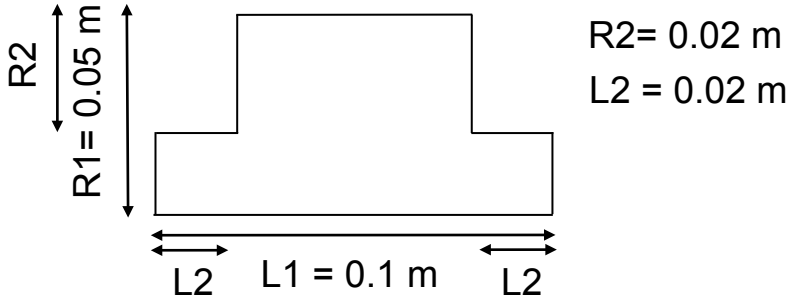

- three cell elliptical cavity

- Verification - comparison with Mafia 2D E-Solver
- Validity check - computed eigenmodes resonate in our time domain solver

Orthogonal properties of the eigenmodes in a cylindrical cavity

For each pair of eigenvectors holds:

$$\int_A \mathbf{H}_\xi \cdot \mathbf{H}_\eta \mathbf{dA} = \sum_i \sum_j h_\xi \cdot h_\eta \Delta z_i \Delta r_j \begin{cases} = 0 & (\xi \neq \eta) \\ \neq 0 & (\xi = \eta) \end{cases}$$

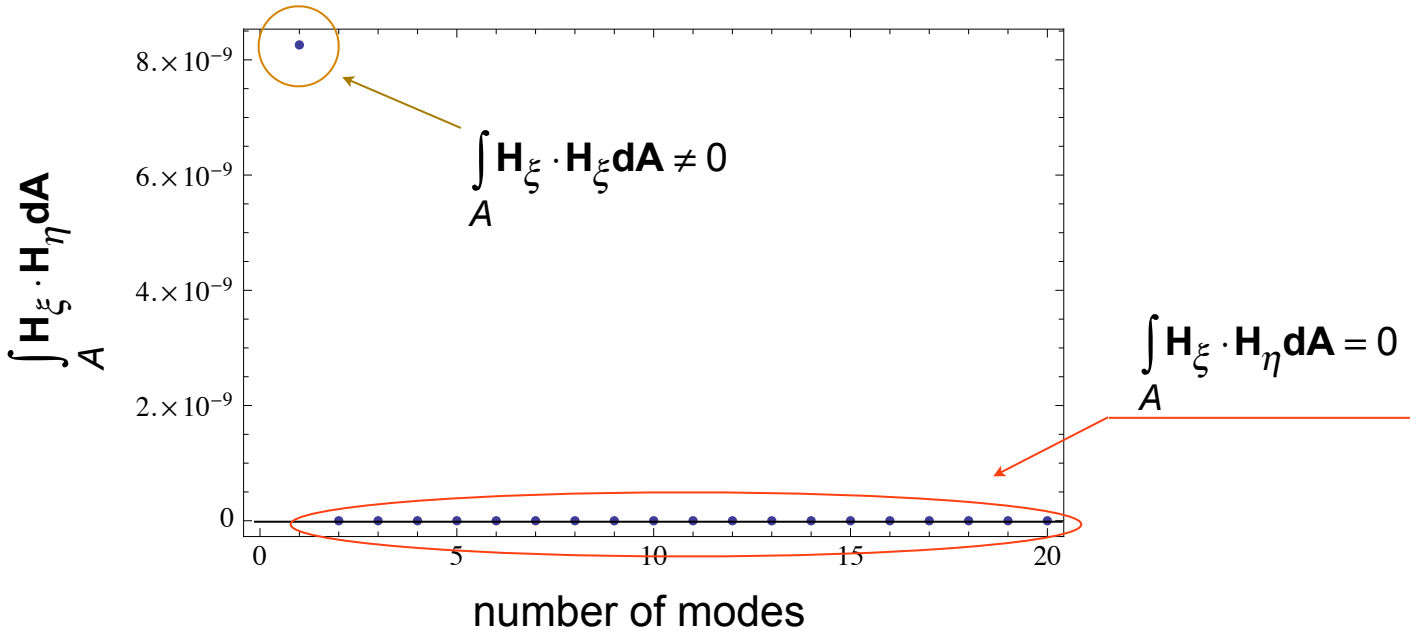

Comparison Mathematica-MAFIA (frequency)

test example:

- cylindrical cavity with a grid resolution of 20,000 grid points

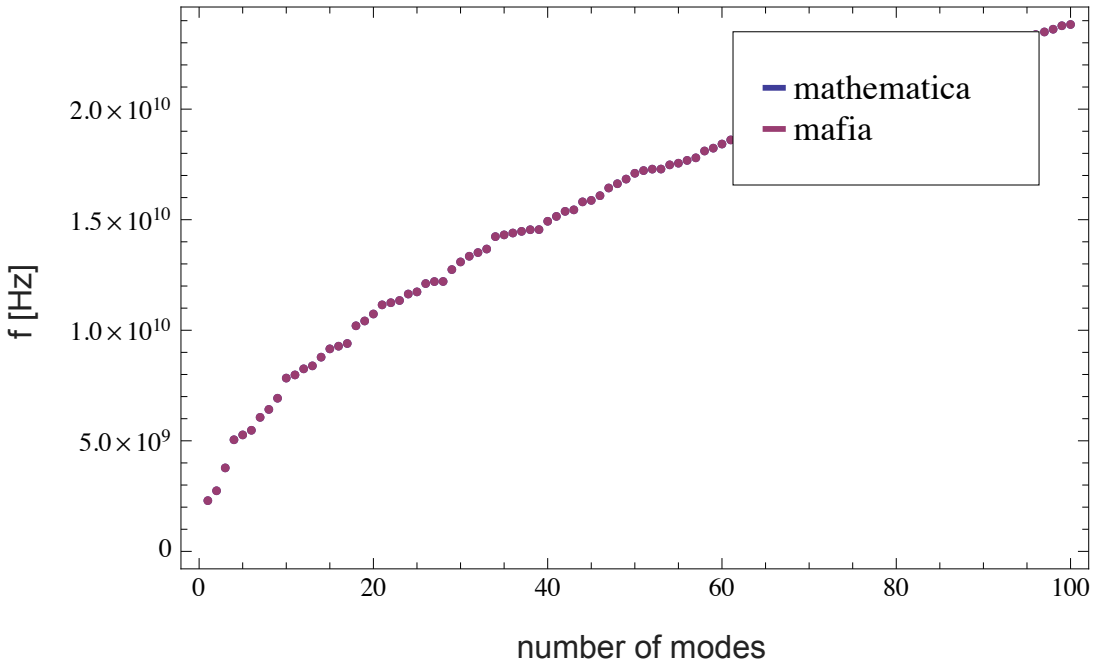

Comparison Mathematica-MAFIA (frequency)

test example:

- cylindrical cavity with a grid resolution of 20,000 grid points

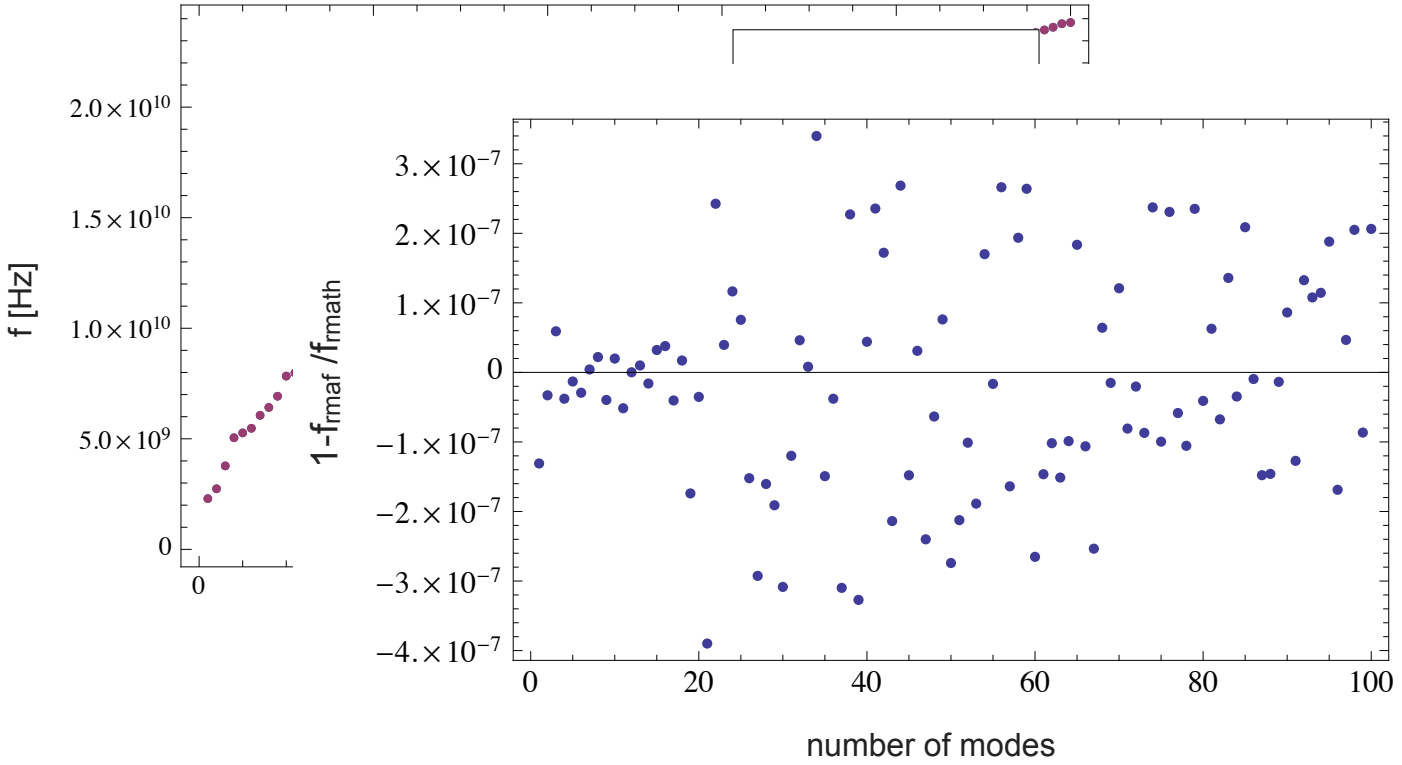

Comparison Mathematica-MAFIA (eigenmode)

Eigenmode solution - black box Mathematica

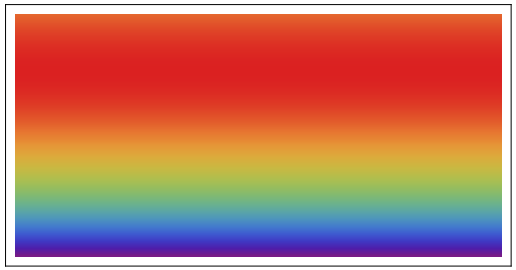

TM_{010}

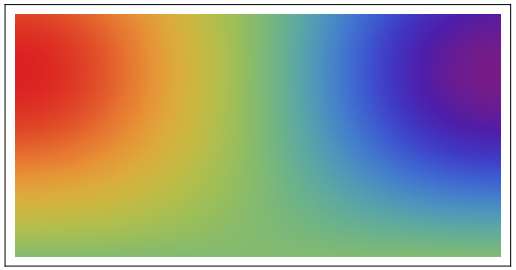

TM_{011}

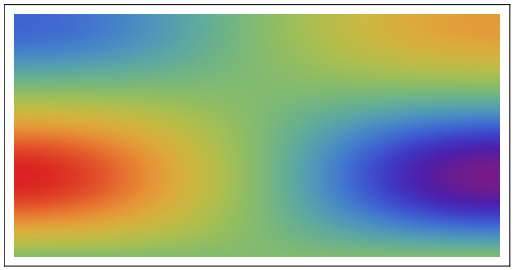

TM_{021}

Comparison Mathematica-MAFIA (eigenmode)

Eigenmode solution - black box Mathematica

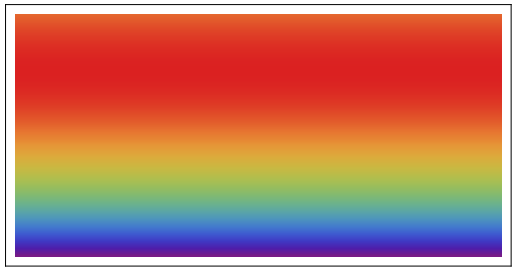

TM_{010}

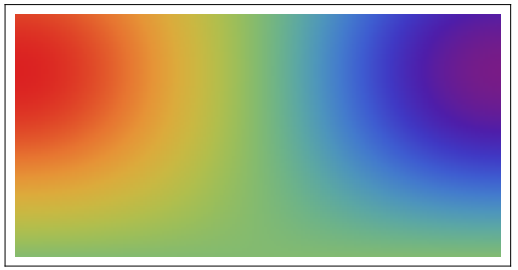

TM_{011}

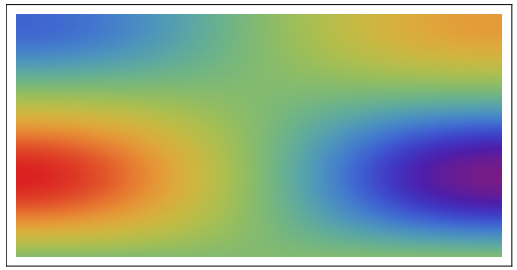

TM_{021}

E-Solver MAFIA

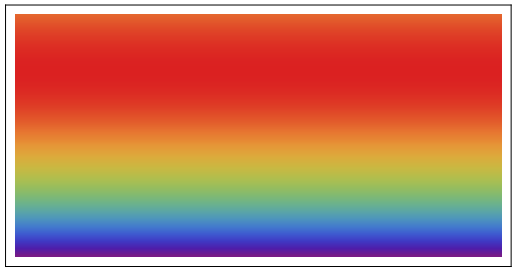

TM_{010}

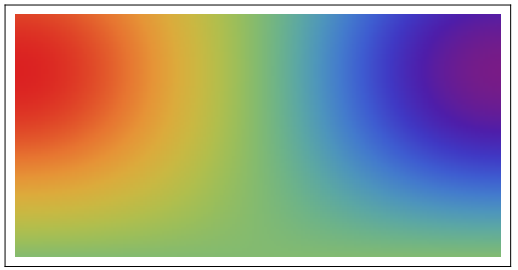

TM_{011}

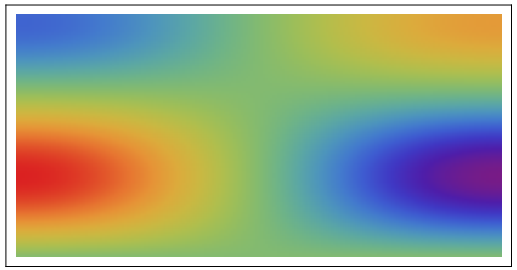

TM_{021}

Plots of 3 eigenmodes (H_φ field)

Comparison Mathematica-MAFIA (eigenmode)

Plot of computation time needed for computation of the first 100 modes studied on different grid resolutions

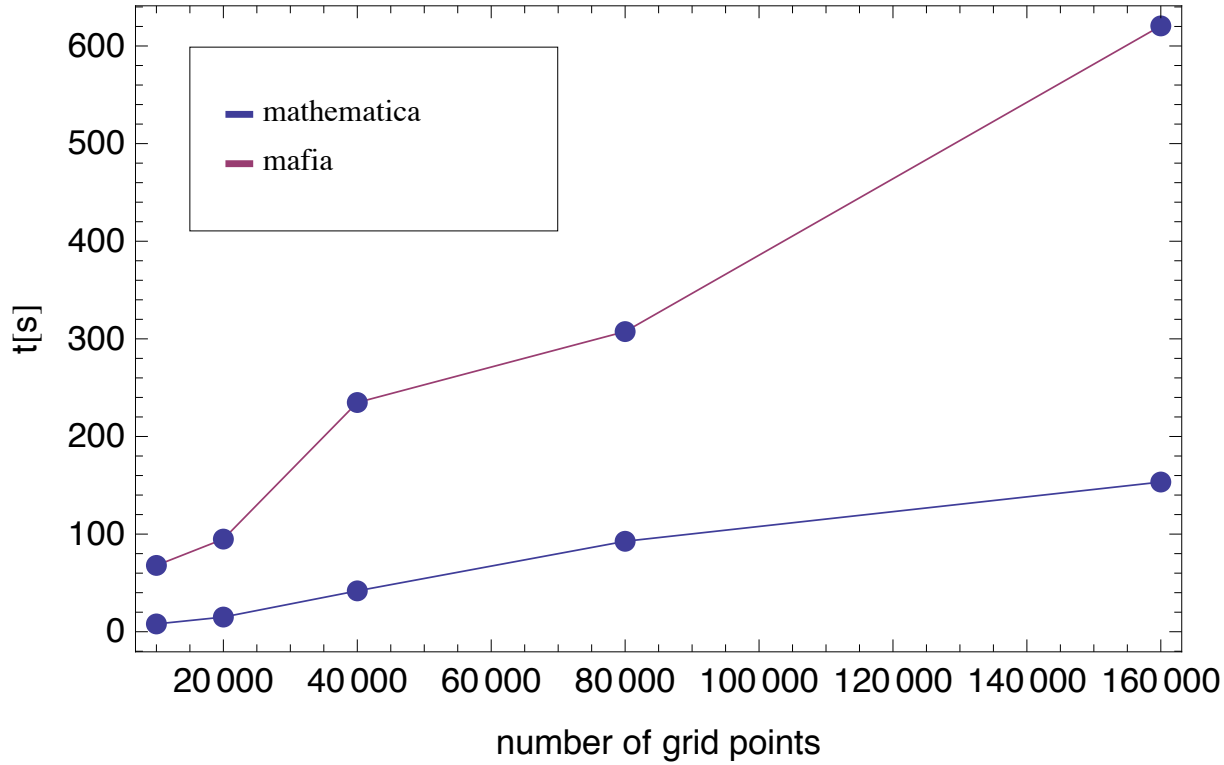

Approach for computing the eigenmodes of realistic structures

Problem of eigenmode computation:

Many zero eigenvalues ⇒ insufficient eigenmode values

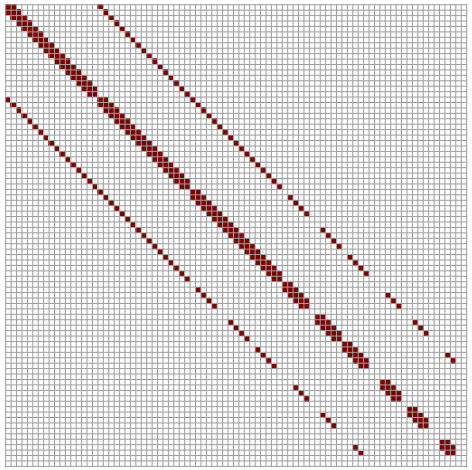

reduce the system matrix -
take out the zero entries

Approach for computing the eigenmodes of realistic structures

Problem of eigenmode computation:

Many zero eigenvalues ⇒ insufficient eigenmode values

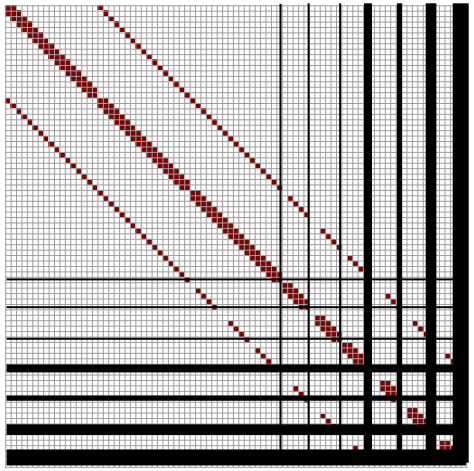

reduce the system matrix -
take out the zero entries

Approach for computing the eigenmodes of realistic structures

Problem of eigenmode computation:

Many zero eigenvalues ⇒ insufficient eigenmode values

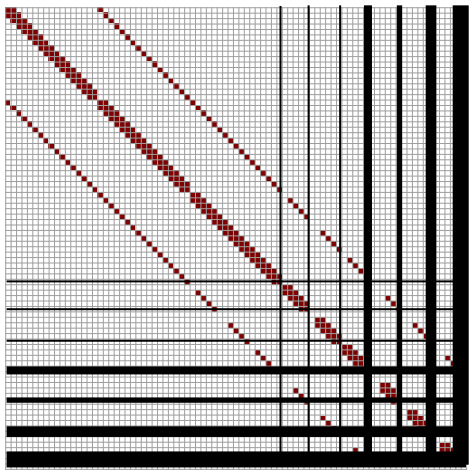

reduce the system matrix - take out the zero entries

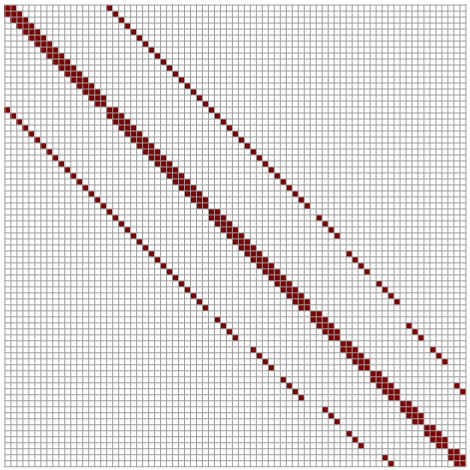

reduced system matrix

Cylindrical pill-box with a beam pipe (20,000 grid points)

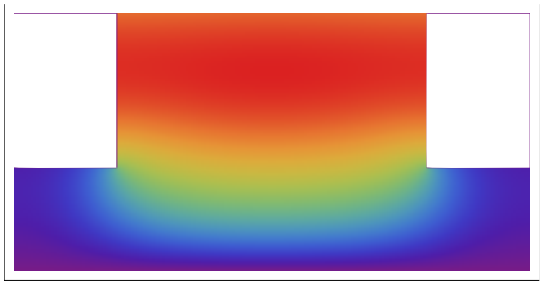

TM_{010}

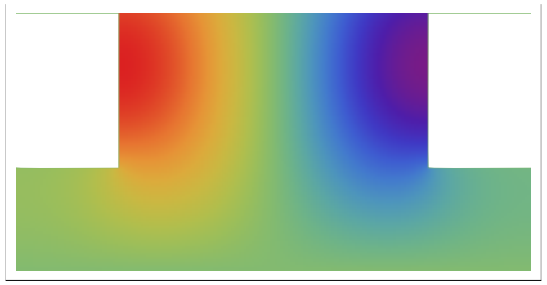

TM_{011}

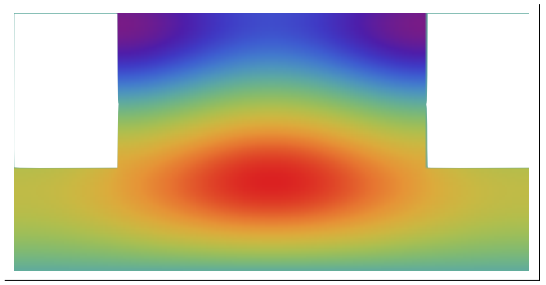

TM_{020}

Ellipsiodal geometrie (315,000 grid points)

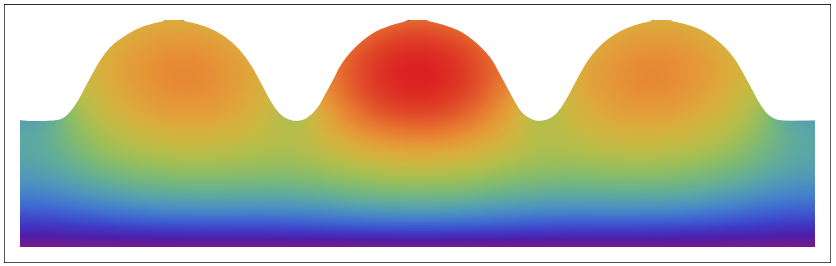

$TM_{010\text{-}0}$

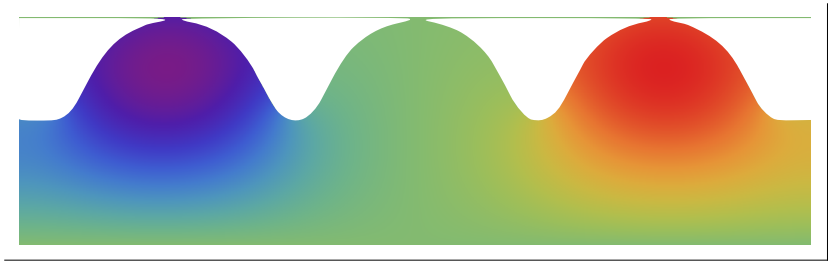

$TM_{010\text{-}\pi/3}$

Plot of H_φ field eigenmodes

Time domain solver

system matrix

$$\begin{pmatrix} \mathbf{I}+\mathbf{T}_{12}\mathbf{T}_{21}+\mathbf{T}_{13}\mathbf{T}_{31} & \mathbf{T}_{12} & \mathbf{T}_{13} \\ \mathbf{T}_{21} & \mathbf{I} & \mathbf{0} \\ \mathbf{T}_{31} & \mathbf{0} & \mathbf{I} \end{pmatrix}$$

start field vector

$$\begin{pmatrix} h_{\varphi}^{0} \\ e_{r}^{0} \\ e_{z}^{0} \end{pmatrix}$$

time step size

Time domain solver

$$\begin{pmatrix} h_{\varphi}^{(n+1)} \\ e_{r}^{(n+1/2)} \\ e_{z}^{(n+1/2)} \end{pmatrix}$$

field vector after n+1 time steps

Comparison Mathematica-MAFIA (Hφ field distribution)

amplitude stable (max. relative difference start - end: $2.95 \cdot 10^{-6}$)
amplitude difference (max. relative difference between programs: $3.83 \cdot 10^{-6}$)

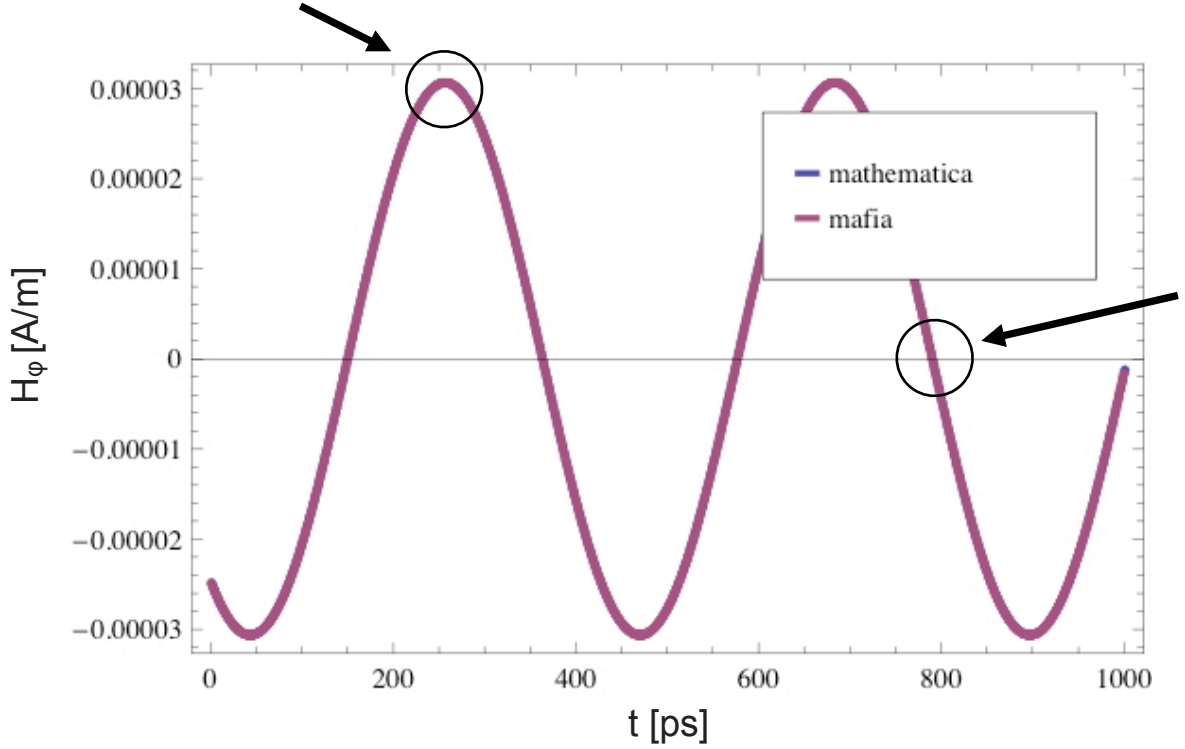

max. absolute phase differente: $7.65 \cdot 10^{-2}$ ps = 0.064 deg

Plot of both curves over the last 1,000 from 5 million time steps
Frequency f = 2.3429 GHz.

Cornell cavity

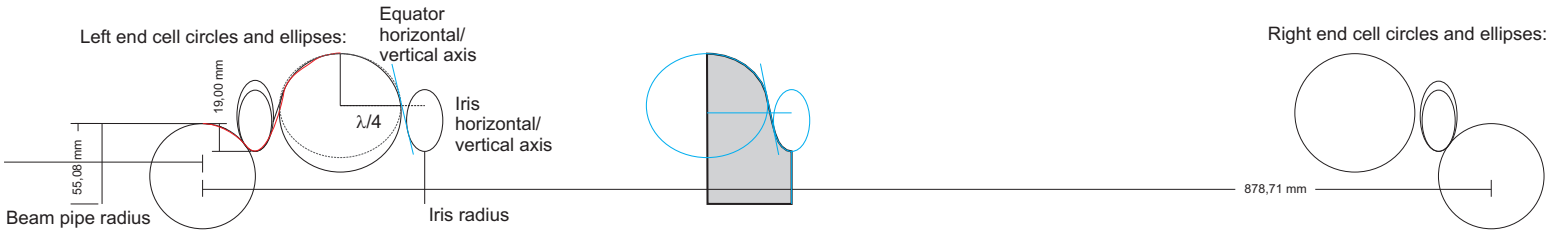

Bild Quelle: Cornell (via HZB)

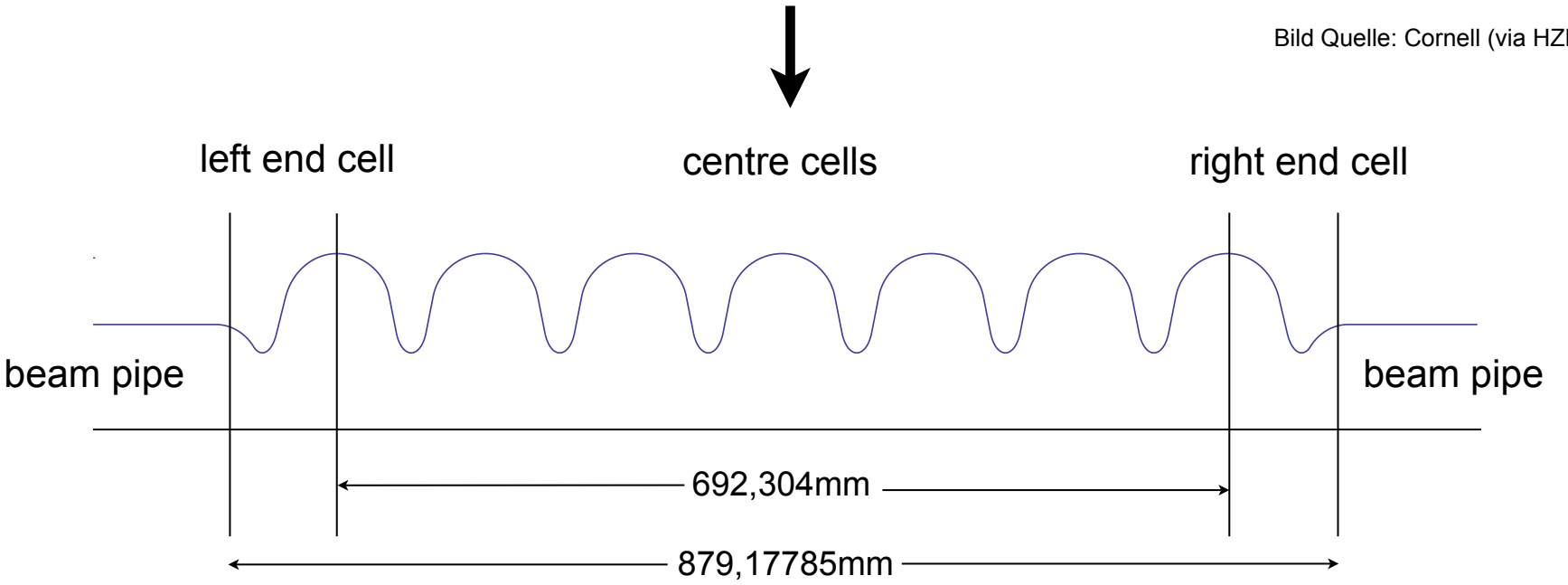

Elliptical half-cell geometry

$$r = \frac{r_2 - r_1}{z_2 - z_1}(z - z_1) + r_1$$

$$r = (r_i + b_i) - b_i\sqrt{1 - \left(\frac{z - z_i}{a_i}\right)^2}$$

$$r = (R_e - B_e) + B_e\sqrt{1 - \left(\frac{z - z_i}{A_e}\right)^2}$$

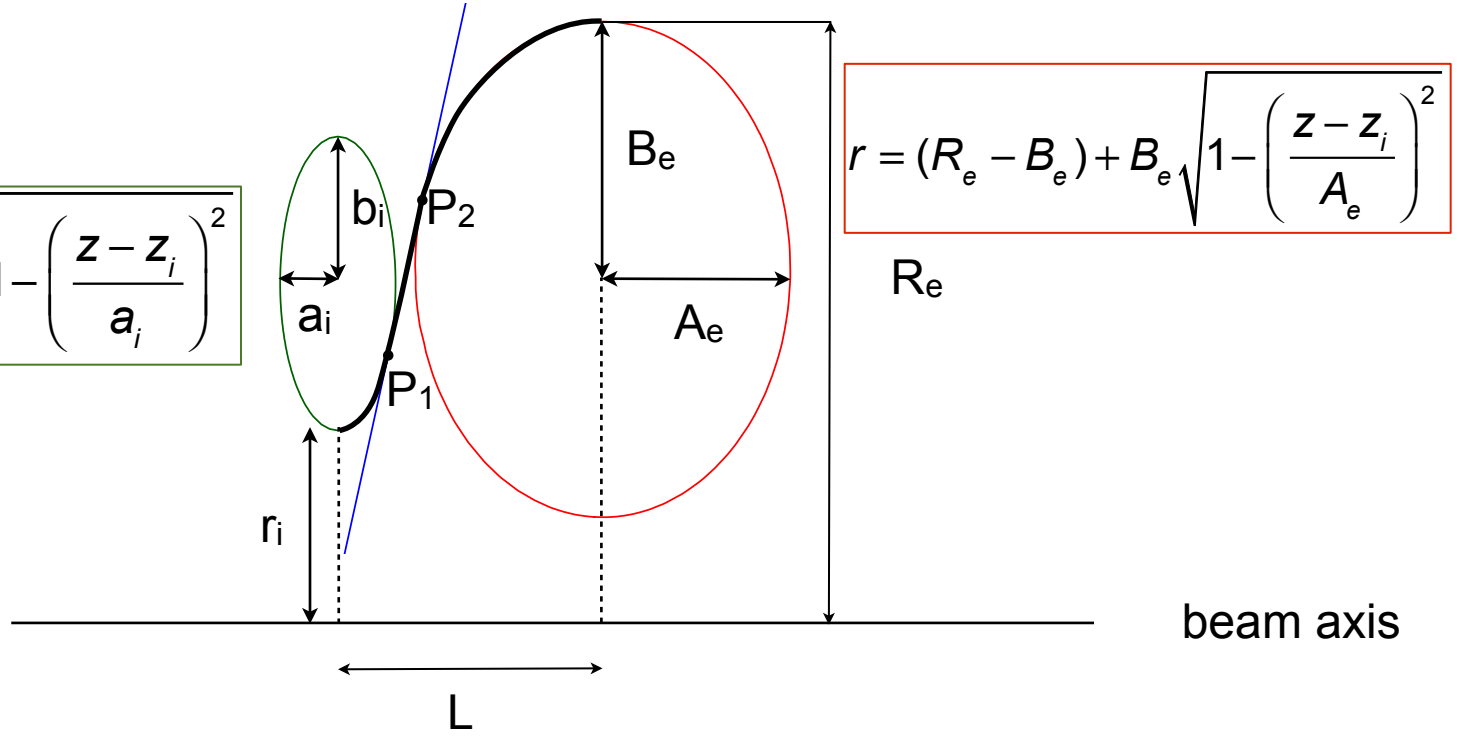

Cornell cavity

Plot of the computational time needed for computation of the first 200 modes studied on different grid resolutions

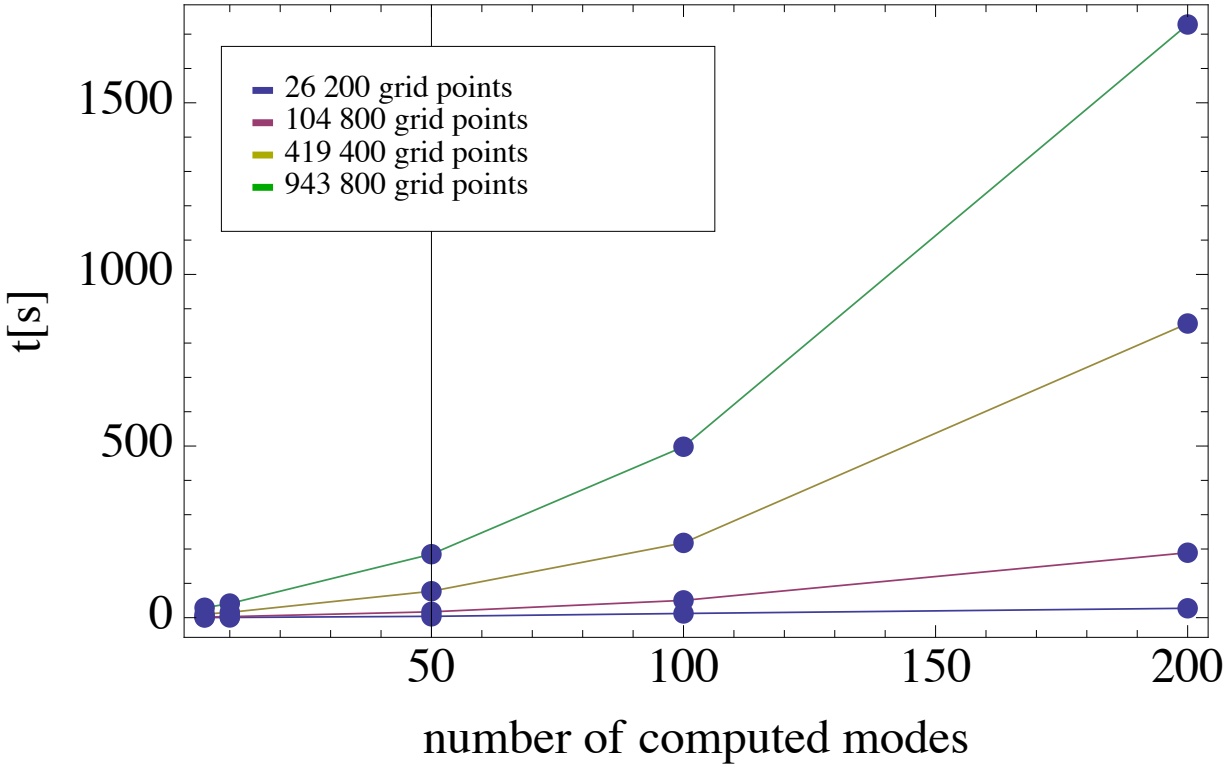

Plot of H_φ, E_z and E_r components of the accelerating mode $TM_{010-\pi}$ with f=1.298853 GHz;

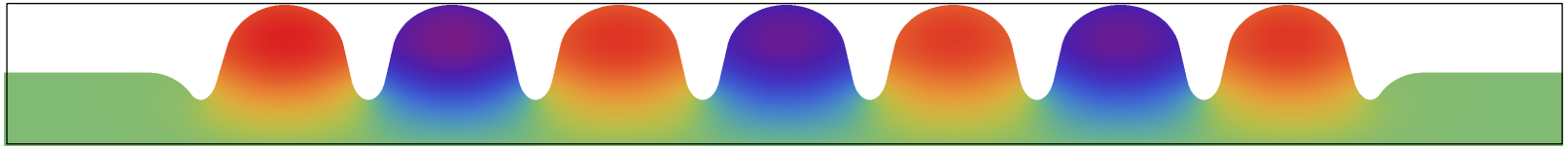

H_φ-component of accelerating mode

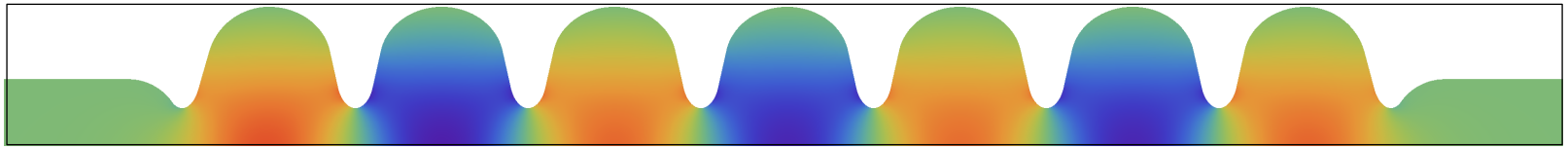

E_z-component of accelerating mode

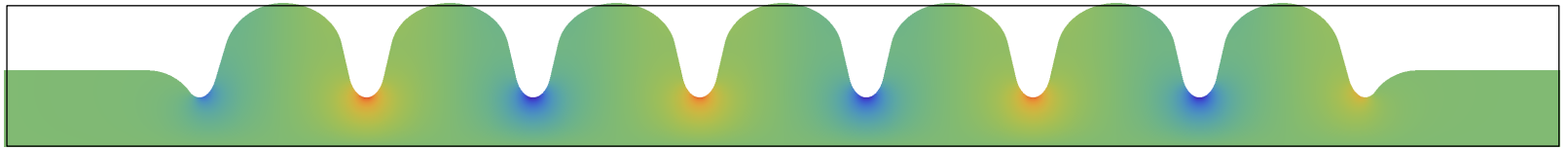

E_r-component of accelerating mode

Computation of the peak electric field

$$E_{peak} = \max(\sqrt{E_z^2 + E_r^2})$$

E_z - electric field in z-direction

E_r - electric field in r-direction

Plot of the E_r field values that lie on the boundary vacuum-PEC

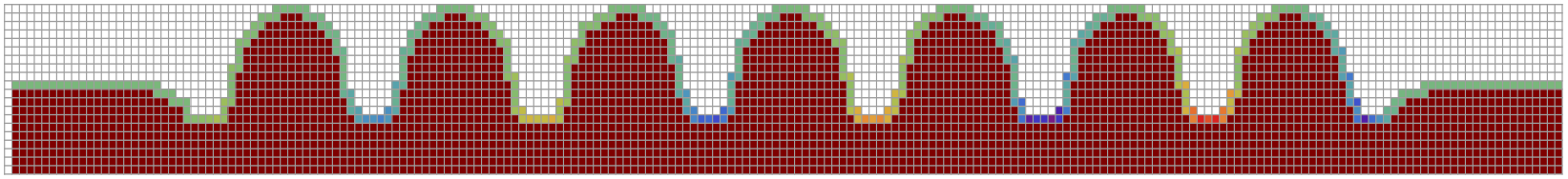

Computation of the peak electric field

$$E_{peak} = \max(\sqrt{E_z^2 + E_r^2})$$

E_z - electric field in z-direction

E_r - electric field in r-direction

Plot of the E_r field values that lie on the boundary vacuum-PEC

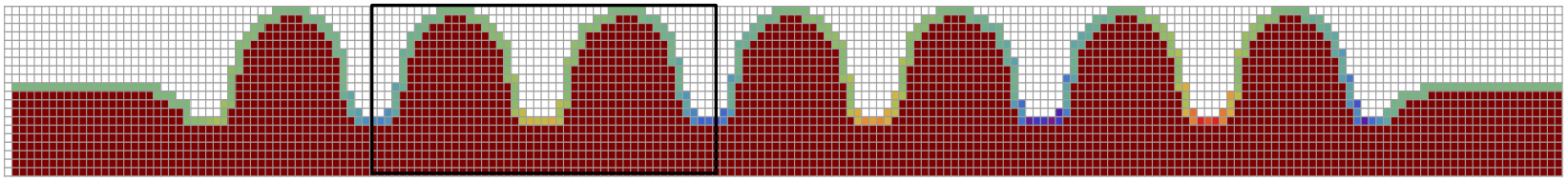

Computation of the peak electric field

$$E_{peak} = \max(\sqrt{E_z^2 + E_r^2})$$

E_z - electric field in z-direction

E_r - electric field in r-direction

Plot of the E_r field values that lie on the boundary vacuum-PEC

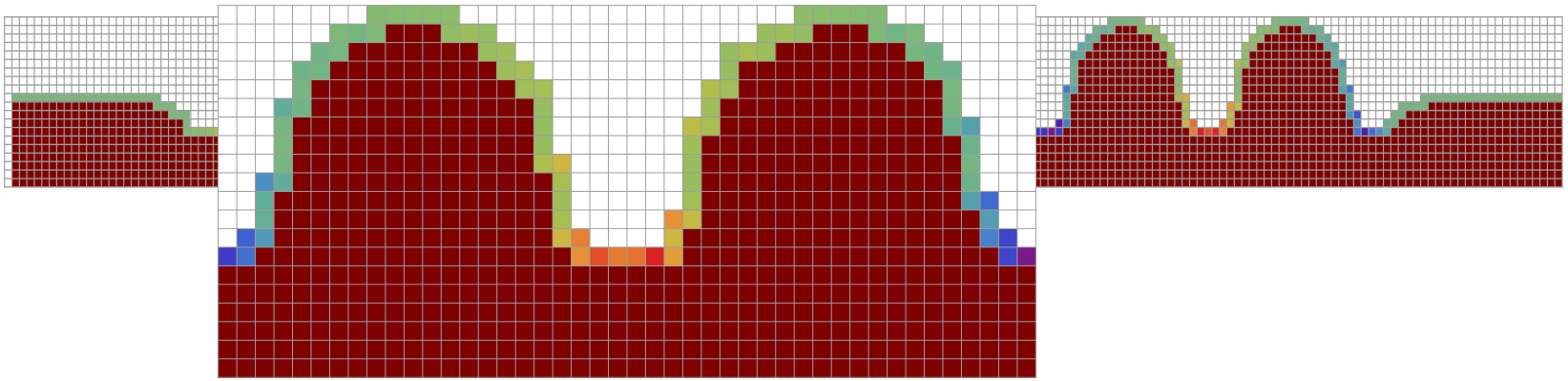

Computation of the peak electric field

$$E_{peak} = \max(\sqrt{E_z^2 + E_r^2})$$

E_z - electric field in z-direction

E_r - electric field in r-direction

Plot of E_r field values that lie on the boundary vacuum-PEC

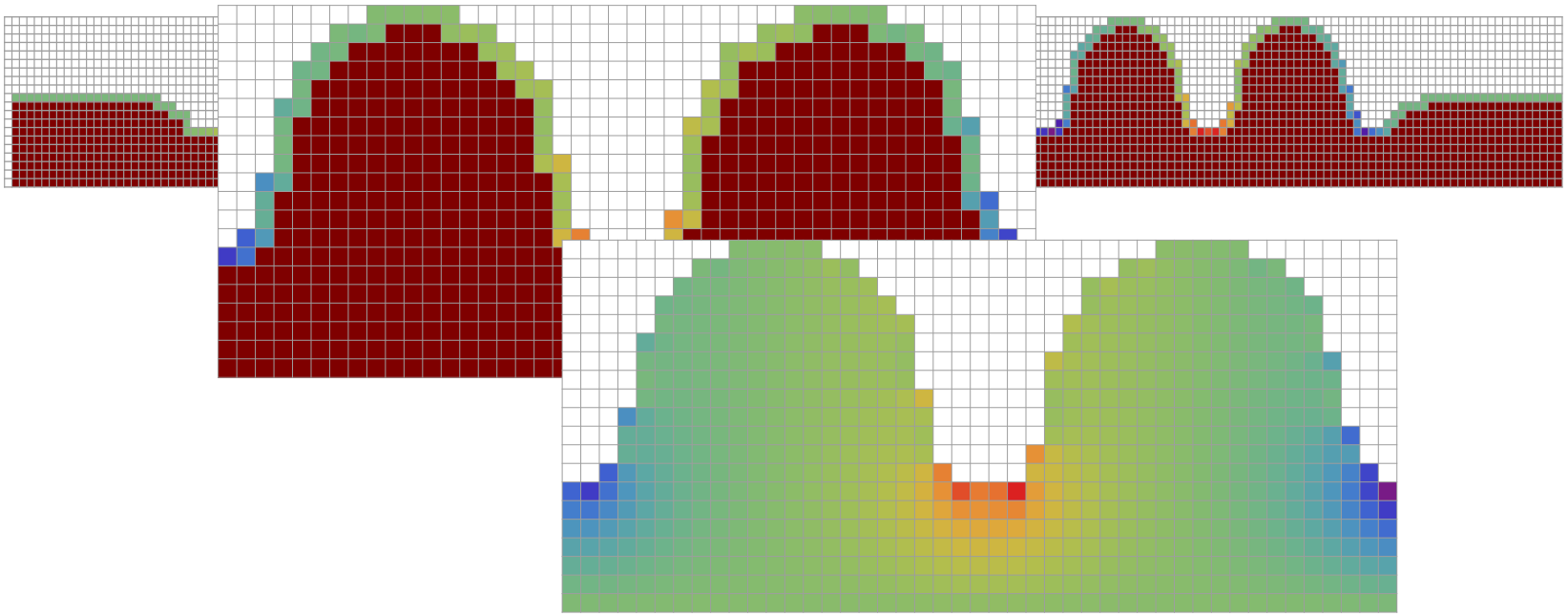

Computation of the accelerating electric field

$$E_{acc} = \frac{1}{L_{cav}} \left| \int_{z=0}^{L_{cav}} E_{z0}(z) \cdot e^{i\omega z / c_0} dz \right| \longrightarrow V_{acc}$$

E_{z0} - longitudinal field

L_{cav} - the length of the cavity

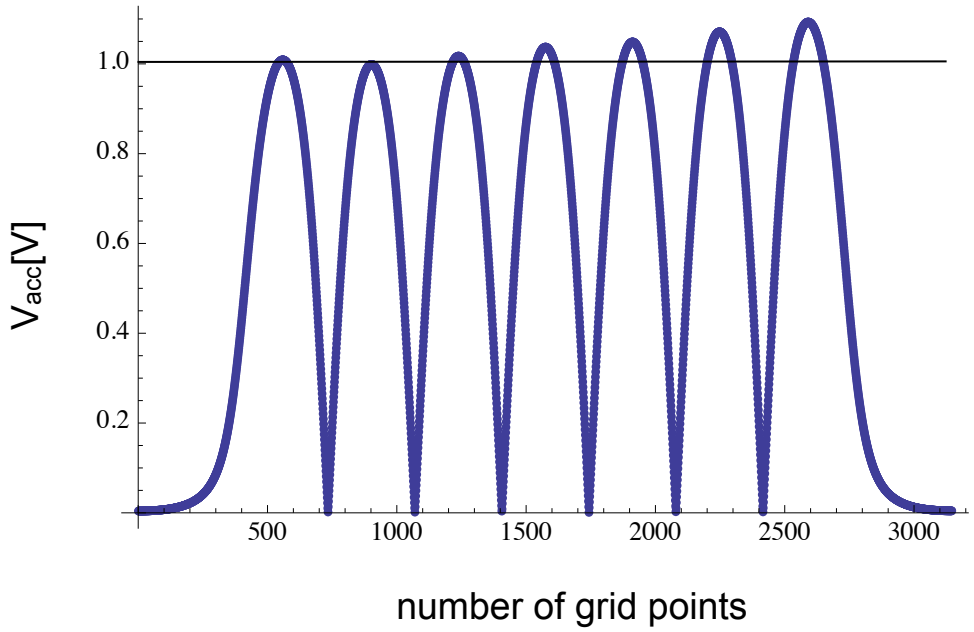

Multicell field flatness tuning (goal: $E_{peak}/E_{acc}\approx 2$)

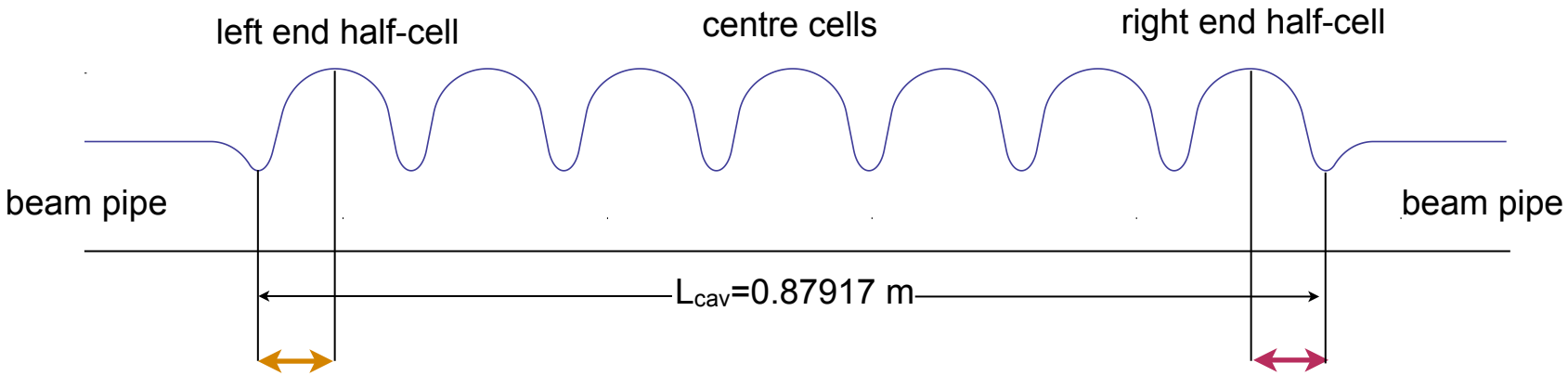

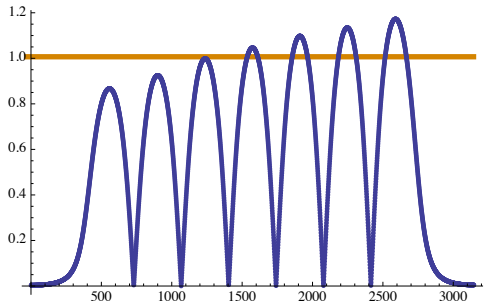

f =1.2987GHz
L_{cav} =0.87887m
E_{peak}/E_{acc} = 3. 5724

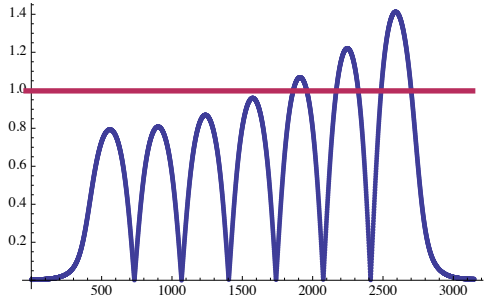

f = 1.29899 GHz
L_{cav} = 0.87973m
E_{peak}/E_{acc} = 4.1704

Multicell field flatness tuning (goal: $E_{peak}/E_{acc}\approx 2$)

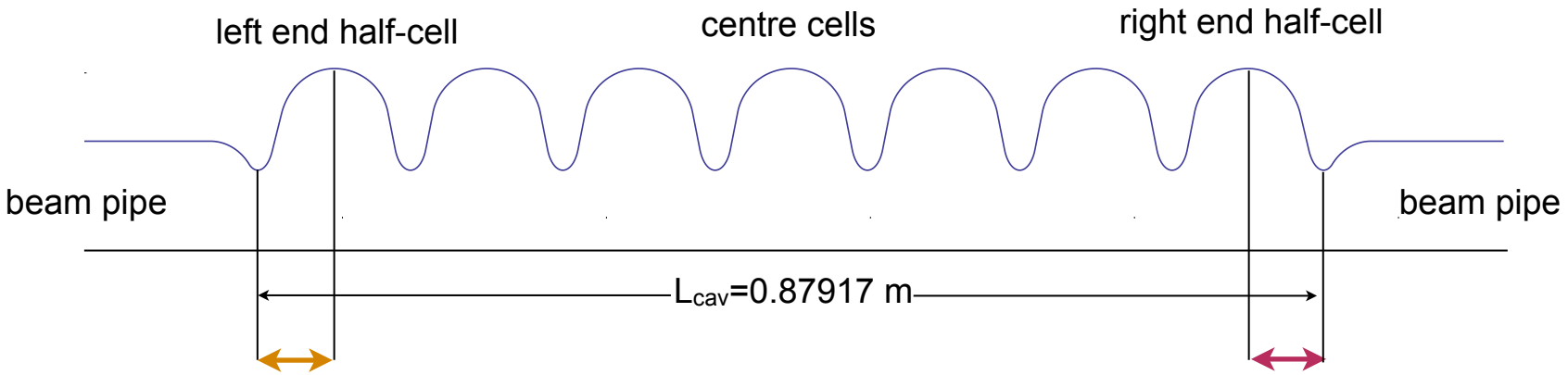

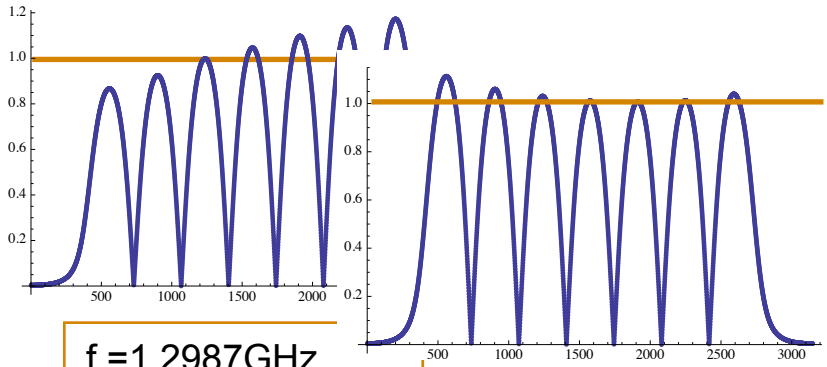

f =1.2987GHz
L_{cav} =0.87887m
E_{peak}/E_{acc} = 3. 5724

f = 1. 29885 GHz
L_{cav} =0.87928m
E_{peak}/E_{acc} = 3. 3881

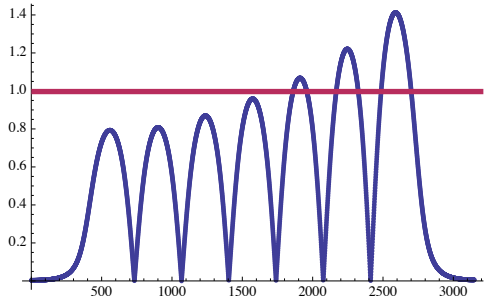

f = 1.29899 GHz
L_{cav} = 0.87973m
E_{peak}/E_{acc} = 4. 1704

Summary

- FIT scheme is applied to fields of rotational symmetry and of TM-type in Mathematica and the code‘s validity is checked in MAFIA
- Code implementation on equidistant and non equidistant grid
- Eigenproblem solution is studied for three different geometries
- Time domain solver is implemented
- Amplitude stays stable and propagation frequency dosen‘t change
- Cavity simulations performed on 7-cell Cornell cavity with aim of cavity optimization